CHEMISTRY
A EUROPEAN JOURNAL

FULL PAPER

DOI: 10.1002/chem.201204035

Protein-Directed Synthesis of Mn-Doped ZnS Quantum Dots: A Dual-Channel Biosensor for Two Proteins

Peng Wu, Ting Zhao, Yunfei Tian, Lan Wu, and Xiandeng Hou*[a]

Abstract: Proteins typically have nanoscale dimensions and multiple binding sites with inorganic ions, which facilitates the templated synthesis of nanoparticles to yield nanoparticle–protein hybrids with tailored functionality, water solubility, and tunable frameworks with well-defined structure. In this work, we report a protein-templated synthesis of Mn-doped ZnS quantum dots (QDs) by exploring bovine serum albumin (BSA) as the template. The obtained Mn-doped ZnS QDs give phosphorescence emission centered at 590 nm, with a decay time of about 1.9 ms. A dual-channel sensing system for two different proteins was developed through integration of the optical responses (phosphorescence emission and resonant light scattering (RLS)) of Mn-doped ZnS QDs and recognition of them by surface BSA phosphorescent sensing of trypsin and RLS sensing of lysozyme. Trypsin can digest BSA and remove BSA from the surface of Mn-doped ZnS QDs, thus quenching the phosphorescence of QDs, whereas lysozyme can assemble with BSA to lead to aggregation of QDs and enhanced RLS intensity. The detection limits for trypsin and lysozyme were 40 and 3 nM, respectively. The selectivity of the respective channel for trypsin and lysozyme was evaluated with a series of other proteins. Unlike other protein sensors based on nanobioconjugates, the proposed dual-channel sensor employs only one type of QDs but can detect two different proteins. Further, we found the RLS of QDs can also be useful for studying the BSA–lysozyme binding stoichiometry, which has not been reported in the literature. These successful biosensor applications clearly demonstrate that BSA not only serves as a template for growth of Mn-doped ZnS QDs, but also impacts the QDs for selective recognition of analyte proteins.

Keywords: biosensors · enzymes · manganese · proteins · quantum dots · zinc sulfide

Introduction

Protein detection is of utmost importance to many fields, including disease diagnosis and proteomic study. Integration of proteins with nanoparticle (NP)-based sensing platforms for analyte proteins has led to significant advances in sensitivity, greatly increased specificity, and enhanced signal transduction through the nanoparticle reporter.[1] In these protein biosensors, the NPs must first be post-functionalized with capture proteins (or DNA, aptamer, and RNA) to provide analyte binding sites for selective determination of targets through specific interactions such as antibody–antigen, enzyme–substrate, DNA–protein, aptamer–target, and lectin–glycoprotein recognition. Such post-functionalization typically relies on 1-ethyl-3-(3-dimethylaminopropy)carbodiimide (EDC)/*N*-hydroxysuccinimide (NHS) coupling,[2] which is usually time consuming and labor intensive. On the other hand, the capture moieties (protein, DNA, or RNA) in the protein sensors possess nanoscale dimensions and constitute the fundamental building blocks of natural systems. Using these biomolecules as natural templates for NP synthesis can directly yield the desired NP–biomolecule hybrids with tailored functionality in one pot.[3] In this vein, biomolecules—including proteins,[4] peptide,[5] DNA,[6] and RNA[7]—have all been employed as templates to ensure water solubility and to impart programmability to the synthesis by providing a tunable framework with a well-defined structure. Exploration of these biomolecules as both template for NP synthesis and a binding location for analyte protein recognition provides a new avenue for protein biosensor design.[8]

In addition to postsynthetic functionalization, previous protein biosensors have typically employed a single signal transduction mode. Thus, only one analyte protein can be detected each time. In fact, NPs often possess more than one-dimensional optical properties, which provides vast potential for multichannel sensing.[9] Mn-doped ZnS QDs,[10] a promising alternative to current cadmium-based QDs, are also promising candidates for multidimensional sensing, given that the defect-related fluorescence and light scattering of the QDs are elegantly modulated together with phosphorescence emission.[11] The exploration of Mn-doped ZnS QDs for multidimensional sensing is still in its infancy stage. For example, the multidimensional sensing capability of Mn-doped ZnS QDs has been explored with small thiol-[11a] and polyethyleneimine-capped QDs.[11b] Natural systems often

[a] Dr. P. Wu, T. Zhao, Y. F. Tian, Dr. L. Wu, Prof. Dr. X. D. Hou
Analytical & Testing Center and Key Laboratory of Green Chemistry and Technology of MOE in College of Chemistry
Sichuan University, Chengdu
Sichuan 610064 (P.R. China)
Fax: (+86) 28-8547-0818
E-mail: houxd@scu.edu.cn

Supporting information for this article is available on the WWW under http://dx.doi.org/10.1002/chem.201204035.

utilize a single protein to perform multiple functions. Control over functional specificity is achieved through interactions with other proteins at well-defined epitope binding sites to form a variety of functional coassemblies. It is thus expected that protein-functionalized Mn-doped ZnS QDs might have great potential for sensing more than one analyte protein with multichannel readouts.

Therefore, we have developed a protein-directed strategy for synthesis of Mn-doped ZnS QDs to yield protein-functionalized QDs in one pot. We chose BSA, the most thoroughly characterized, inexpensive, and ubiquitous plasma protein, as the template for synthesis of Mn-doped ZnS QDs. Through modulation of the surface ligand coverage density by means of the digestion of BSA by trypsin, and self-assembly of QDs through BSA–lysozyme interactions, a phosphorescent and resonant light scattering (RLS) dual-channel sensing system was developed for biosensing of trypsin and lysozyme. It should be noted that a BB-TrxA:CT43 protein has already been employed for the synthesis of doped ZnS QDs,[12] but the analytical applications have not yet been fully explored. In this work, due to exploration of the multichannel optical properties of Mn-doped ZnS QDs and multivalent recognition of analyte proteins by BSA, the sensing potential of QDs was largely expanded. That is, by using only one type of QDs, two different proteins were quantitatively detected.

Results and Discussion

Design of the synthesis of Mn-doped ZnS QDs and dual-channel sensing scheme for two proteins: In this work, we employed a protein-directed route[12] for the synthesis of Mn-doped ZnS QDs with BSA as the template (Scheme 1). For the synthesis of Mn-doped ZnS QDs, BSA was firstly chemically denatured (see the Supporting Information) to yield denatured BSA (dBSA), which contains 37 thiol groups per monomer and is frequently employed as a template for the synthesis of a variety of NPs.[13] The cation precursors (Zn^{2+} and Mn^{2+}) were then biomineralized with dBSA to form the protein–metal complexes, predominantly through the coordination facility of thiol and amine groups in the protein backbone. After the addition of Na_2S, highly luminescent Mn-doped ZnS QDs were formed in place of these previous complexes (Figure 1a).

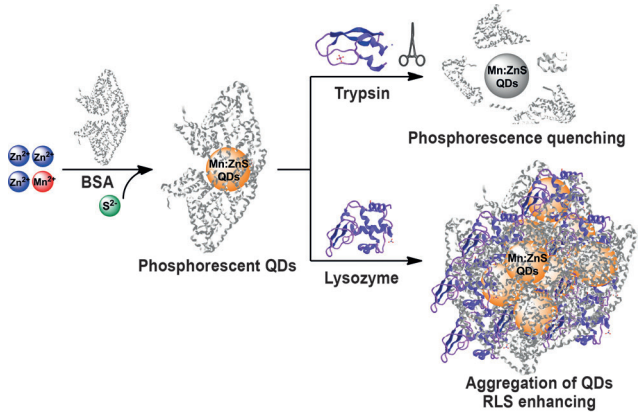

Scheme 1. Protein-directed synthesis of phosphorescent Mn-doped ZnS QDs for dual-functional sensing: phosphorescent sensing for trypsin and RLS sensing for lysozyme.

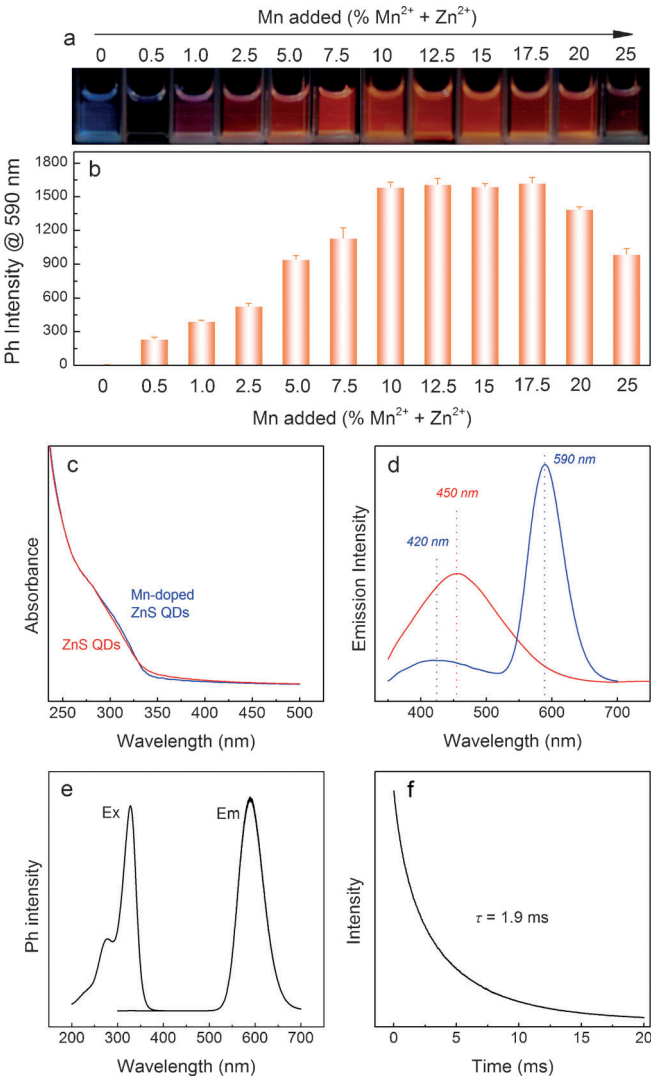

Figure 1. a) Fluorescent photographs of UV-excited dBSA-coated Mn-doped ZnS QDs with increasing Mn^{2+} concentration ($\lambda_{ex}=302$ nm). b) Phosphorescence intensity of Mn-doped ZnS QDs at 590 nm mineralized in the presence of indicated amount of Mn^{2+} ($\lambda_{ex}=280$ nm). c) UV/Vis absorption and d) fluorescence emission spectra of Mn-doped ZnS QDs mineralized in the absence (red) and presence (blue) of 12.5% Mn^{2+}. e) Phosphorescent excitation and emission spectra, and f) phosphorescent decay curve of Mn-doped ZnS QDs (12.5% Mn^{2+}).

The dual-channel sensing strategy for proteins with dBSA-templated Mn-doped ZnS QDs is shown in Scheme 1. The physical mechanisms of phosphorescence and RLS are totally different: phosphorescence originates from the photoexcitation of the ZnS host, followed by rapid energy transfer from ZnS to the triplet transition ($^4T_1 \rightarrow {}^6A_1$) of Mn^{2+}

dopants, whereas RLS can be ascribed to the scattering of incident light by dBSA-coated QDs. By taking advantage of the role of ligands on the emission of QDs[14] and the digestion of proteins by protease, the phosphorescent channel was explored for trypsin biosensing through phosphorescence quenching. Lysozyme was reported to assemble with serum albumin.[15] We hypothesize that when BSA is covered on the surface of QDs, the assembly between BSA and lysozyme would still exist, thus leading to aggregation of QDs and enhancing the RLS. Therefore, the RLS channel was utilized for lysozyme sensing through RLS enhancement. Such a dual-channel sensing system revolutionizes the conventional sensing scheme, that is, it employs only one type of QDs but can detect two different proteins.

Optimization and characterization of the Mn-doped ZnS QDs: The synthetic conditions of dBSA-capped Mn-doped ZnS QDs were investigated in detail (see the Supporting Information). To investigate the optimal doping amount of Mn^{2+}, various amounts of $Mn(Ac)_2$ were added to the $ZnAc_2$ electrolyte in the presence of dBSA; the total cation amount ($Zn^{2+}+Mn^{2+}$) was kept at 0.25 mmol. As shown in Figure 1a, the emission color of the QDs changed immediately after incorporation of Mn^{2+}, and the optimal amount of Mn^{2+} was found to be in the range of 10–17.5% (Figure 1b). The exactly incorporated amounts of Mn^{2+} into the ZnS host almost mirrored the solution chemistry (as analyzed by inductively coupled plasma optical emission spectrometry (ICP-OES) and summarized in Table S1 of the Supporting Information). In conventional synthesis of Mn-doped ZnS QDs, doping into host QDs is difficult (<5% dopant amount) owing to the possible "self-purification" effect of the host.[16] In this work, however, the doping amounts were significantly higher. It is possible that protein-templated synthesis yields a better microenvironment for dopant incorporation.[12] However, why such larger amounts of Mn^{2+} are required to achieve higher phosphorescence remains unclear at present, probably due to an idiosyncrasy of the protein-templated synthesis process.[12]

After optimization of the synthetic conditions (see the Supporting Information), QDs biofabricated in the presence of 12.5% Mn^{2+} were selected for detailed characterization. XRD measurements confirmed the typical zinc blend structure of the as-synthesized Mn-doped ZnS QDs (Figure 2a). The absorption edges of doped and undoped ZnS QDs were located at 335 and 330 nm, respectively (Figure 1c). According to the high-resolution (HR) TEM measurements, the roughly spherical QDs had an average diameter of (3.8±0.4) nm (Figure 2b and Figure S3 in the Supporting Information). Emission spectra revealed that Mn doping resulted in blueshifting of the defect emission of ZnS from 450 to 420 nm. Meanwhile, the intensity of such defect emission of ZnS was significantly quenched upon Mn doping to the benefit of a new emission peak centered at 590 nm (Figure 1d). This is fully consistent with doping of Mn^{2+} into the ZnS lattice and energy transfer from the conduction band of ZnS to the $^4T_1\rightarrow{}^6A_1$ Mn^{2+} transition.[17] Because of the triplet

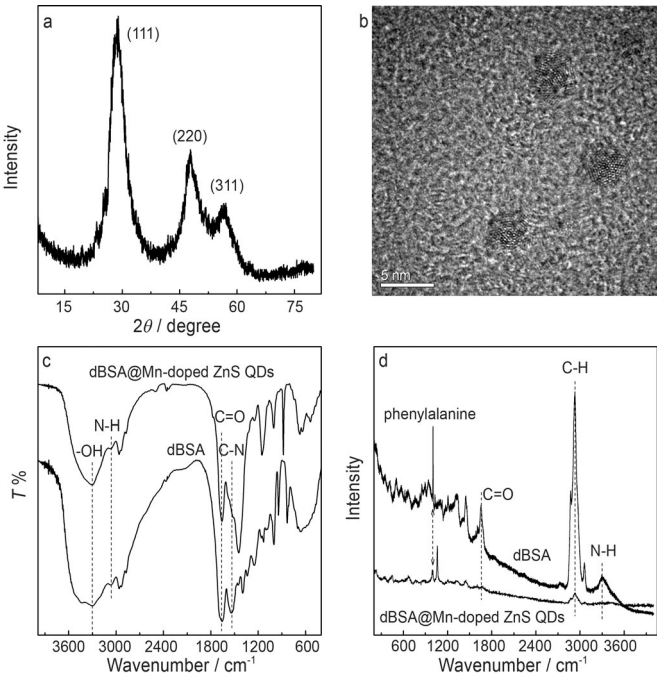

Figure 2. Characterization of dBSA-coated Mn-doped ZnS QDs. a) XRD, b) HRTEM (scale bar 5 nm), c) FTIR, and d) FT-Raman spectra of dBSA and dBSA-coated Mn-doped ZnS QDs.

nature of the Mn^{2+} $^4T_1\rightarrow{}^6A_1$ transition, the newly occurred dopant emission (centered at 590 nm) can be observed in phosphorescent detection mode (Figure 1e) with a decay time of about 1.9 ms (Figure 1f), whereas the defect emission (centered at 420 nm) completely disappeared, and this is similar to the previous findings.[10b,e,f,11]

The dBSA-capped Mn-doped ZnS QDs were also characterized by using FTIR and FT-Raman spectroscopy. As shown in Figure 2c, The IR signals of pure dBSA at 3300, 3062, 1652, and 1531 cm^{-1} could be assigned to the stretching vibration of OH, amide A (mainly N–H stretching vibrations), amide I (mainly C=O stretching vibrations), and amide II (the coupling of the bending vibration of N–H and the stretching vibration of C–N) bands, respectively. Most of the characteristic signals of dBSA could be found in the spectra of dBSA-capped Mn-doped ZnS QDs except for amide II. Besides, the absorption of OH or C=O was appreciably decreased. Considering that there are 37 thiols in the dBSA structure, the adhesion of Mn-doped ZnS QDs to dBSA was mainly through the thiol, amine, and carboxyl groups.[18] Raman spectra characterization also confirmed the above interactions (Figure 2d).

The as-synthesized dBSA-capped Mn-doped ZnS QDs were physically and optically stable for at least six months when stored at 4 °C in the original synthesis media. Another appealing feature of dBSA-capped Mn-doped ZnS QDs is that they could remain stable in as high as 1 M NaCl media ($\Delta Ph<5\%$), whereas the conventional mercaptoproponic acid (MPA)-capped Mn-doped ZnS QDs could only withstand 50 mM NaCl media (Figure S4 in the Supporting Infor-

mation),[11a] thereby highlighting the advantage of protein coating. Investigation of pH stability indicated that dBSA-capped Mn-doped ZnS QDs favor applications in the physiological pH range (Figure S4 in the Supporting Information). Such features indicate that dBSA-capped Mn-doped ZnS QDs might be quite suitable for applications in biological media.

Phosphorescent sensing of trypsin: It is well known that surface ligands are of vital importance to the luminescence of QDs.[14] The as-prepared dBSA-coated Mn-doped ZnS QDs were first employed as a phosphorescent sensor for trypsin on the basis of specific cleavage of BSA by trypsin. Trypsin is one of the most important digestive enzymes and is produced in the pancreas as the inactive proenzyme trypsinogen. It is a class of protease that is involved in many normal biological processes as well as diseases, including cancer, stroke, and infection.[19] Ubiquitous in nature, proteases are present in all living cells and organisms, and are known to play a pivotal role in the development and control of many biological processes. In fact, proteolytic activity is sometimes used as a marker for some types of cancer.[20] In proteomics studies, trypsin is also frequently employed for the degradation of proteins into peptides. In view of the vital importance of trypsin, new convenient assays for trypsin detection are highly desired for the development of efficient diagnostic and therapeutic methods. In fact, trypsin assays with QDs have been reported, the majority of which are based on detection schemes of fluorescence resonance energy transfer (FRET),[21] in which the conjugation of QDs and chromophores with specific peptides or proteins are required. The as-prepared dBSA-coated Mn-doped ZnS QDs in this work can be directly engineered into a phosphorescent biosensor for trypsin, thereby eliminating multiple processing steps such as centrifugation and purification.

As shown in Figure 3a, upon addition of trypsin, the phosphorescence of QDs was gradually quenched. Control experiments with MPA-capped Mn-doped ZnS QDs showed that trypsin caused phosphorescence improvement (but to a very limited level), thus indicating that phosphorescence quenching in dBSA-coated Mn-doped ZnS QDs system is due to trypsin-induced protein cleavage. Moreover, in the presence of 10 μM trypsin, white turbid species were visualized in the solution of QDs, which could be ascribed to heavy digestion of the protein ligand and subsequent aggregation of Mn-doped ZnS QDs (Figure S4 in the Supporting Information). The quenched phosphorescence intensity of QDs versus the trypsin concentration was linear in the range of 0.1–1.2 μM (Figure 3b), with a limit of detection (LOD) of 0.04 μM.

The selectivity of this phosphorescent assay for trypsin was evaluated with a series of other proteins. As shown in Figure 3c, only trypsin can quench the phosphorescence of dBSA-coated Mn-doped ZnS QDs, whereas no clear decrease in phosphorescence intensity was observed with glucose oxidase (GOx), ovalbumin, pepsin, human serum albumin (HSA), papain, or lysozyme, thus demonstrating the selectivity of enzyme cleavage of dBSA by trypsin. Such a biosensor design for enzyme detection could be extended to other protein–enzyme pairs through templated synthesis of Mn-doped ZnS QDs with corresponding substrate proteins.

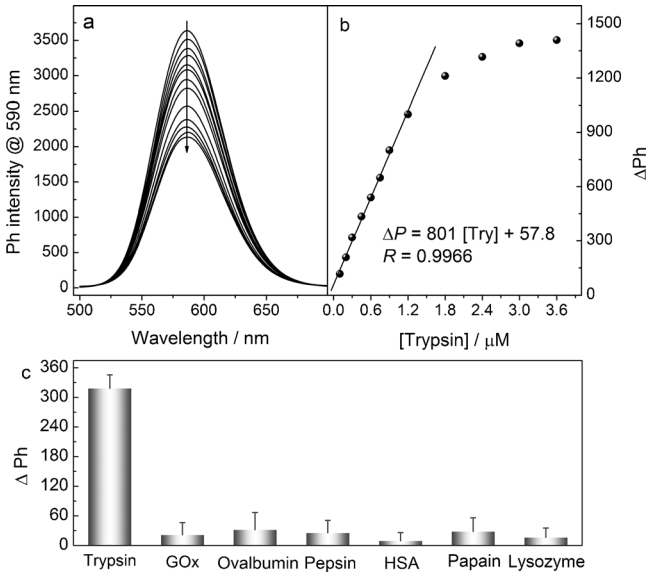

Figure 3. a) Phosphorescence spectra of Mn-doped ZnS QDs in the presence of various concentrations of trypsin. b) Calibration curve and c) selectivity of the dBSA-capped Mn-doped ZnS QDs as a phosphorescent probe for trypsin. Experimental conditions: pH 8.9 PBS buffer, and λ_{ex} = 280 nm.

The potential application of the developed phosphorescent probe was evaluated for determination of trypsin in four urine samples (from healthy volunteers). No phosphorescence background from urine samples was observed, although the fluorescence background was significant (Figure S5 in the Supporting Information), thus demonstrating the superiority of phosphorescent detection over the fluorescent mode. No trypsin was found in these urine samples. The analytical recoveries for spiking 0.3 μM of trypsin ranged from 95.4 to 104% (Table S2 in the Supporting Information). It should be noted that the average urine trypsin level of patients is as high as 84.4 $\mu g\,mL^{-1}$ (3.6 μM).[22] The proposed phosphorescent assay thus holds analytical potential for future clinical diagnosis.

RLS sensing of lysozyme: RLS signals from nanoparticles (NPs) are extremely promising for bioanalysis due to their simplicity and sensitivity. Enhanced RLS signals from NP aggregates induced by analytes can be used for monitoring of molecular interaction or quantitative detection of analytes.[23] In this work, the RLS channel of the as-synthesized Mn-doped ZnS QDs was employed for the biosensing of lysozyme by use of the assembly between BSA and lysozyme.[15a] Lysozyme is an important defense molecule of the innate immune system and one of the major proteins in saliva. The clinical significance of lysozyme is associated with monocytic and monomyelocytic leukemia, tuberculosis, and acute bacterial infections.[24] Previously, aptamers have

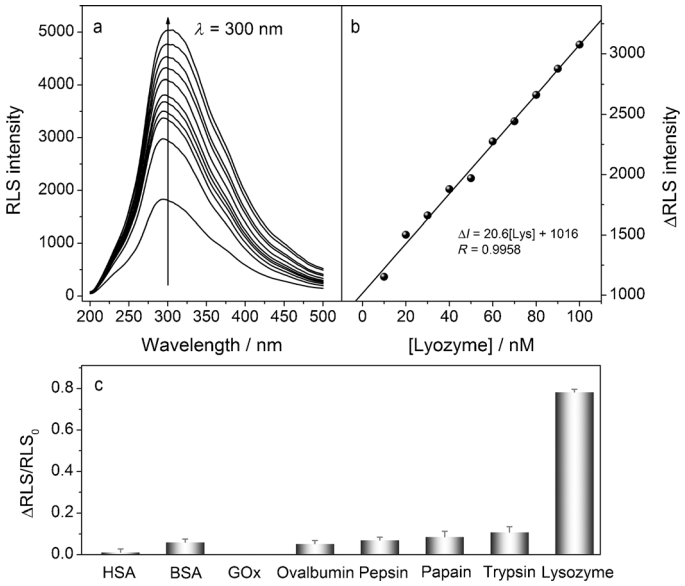

Figure 4. a) RLS spectra of dBSA-coated Mn-doped ZnS QDs in the presence of various concentrations of lysozyme. b) Calibration curve and c) selectivity of the dBSA-capped Mn-doped ZnS QDs as a RLS biosensor for lysozyme (0.3 μM each). Experimental conditions: pH 6 PBS buffer containing 0.2 M NaCl, excitation (ex) and emission (em) slits of 5 nm, and PMT voltage of 400 V.

been frequently employed for biorecognition of lysozyme,[25] whereas the specific recognition of lysozyme by serum albumin has seldom been reported.[15]

As shown in Figure 4a, in the presence of lysozyme, the RLS intensity of dBSA-coated Mn-doped ZnS QDs was gradually enhanced. Because of the specific assembly of BSA and lysozyme,[15] aggregation of dBSA-coated Mn-doped ZnS QDs was formed in the presence of lysozyme, which could be visualized with TEM images (Figure S3c and Figure S3d in the Supporting Information). From the pI of BSA (4.7) and lysozyme (11.0), it seems that the electrostatic effect might be the driving force for assembly of BSA and lysozyme. Investigation of the pH dependence of this assay for lysozyme detection also seems to confirm such a conclusion (Figure 5a). Maximum RLS intensity was obtained at pH 6, at which BSA is negatively charged and lysozyme is positively charged. However, we found that the formation of the QDs aggregates was less affected by the increased ionic strength: the RLS intensity of the QDs aggregates was decreased in the NaCl concentration range of 0–0.2 M, but then leveled off when further increasing the NaCl concentration (even up to 2 M; Figure 5b). From the above results, it can be concluded that, in addition to an electrostatic effect, other types of molecular recognition must exist between BSA and lysozyme,[26] which account for the unaffected ionic strength dependence of aggregation of dBSA-coated Mn-doped ZnS QDs by lysozyme at high NaCl concentration range (Figure 5b). To maximize the performance of the RLS assay for lysozyme, 0.01 M pH 6 PBS buffer that contained 0.2 M NaCl was chosen as the lysozyme biosensor working media. Under the optimized conditions, the RLS intensity of dBSA-coated Mn-doped ZnS QDs versus the concentration of lysozyme was linear in the range of 10–100 nM (Figure 4b) with an LOD of 3 nM. Control experiments showed that the RLS assay can also work with BSA alone as the RLS probe, but the sensitivity was at least three orders of magnitude lower than that with dBSA-coated Mn-doped ZnS QDs (Figure S6 in the Supporting Information), thus demonstrating the superiority of the QD-based RLS assay. The selectivity of the RLS assay for lysozyme was evaluated with several other proteins (HSA, BSA, GOx, ovalbumin, pepsin, papain, and trypsin). As shown in Figure 4c, all of these proteins can cause RLS improvement more or less, but lysozyme gives a much higher response, thus demonstrating the validity of this RLS assay for lysozyme detection. As discussed above, the selectivity should be ascribed to the selective assembly of BSA and lysozyme.

The analytical potential of the RLS probe was evaluated through determination of lysozyme in pharmaceutical tablets. After proper sample preparation (see the Supporting Information), the extraction solutions of the pharmaceutical tablets were analyzed with the RLS probe; good agreements were achieved between the analytical results and the labeled values (Table S3 in the Supporting Information). The analytical recoveries for spike-recovery tests ranged from 99.6 to 108 % (Table S3 in the Supporting Information).

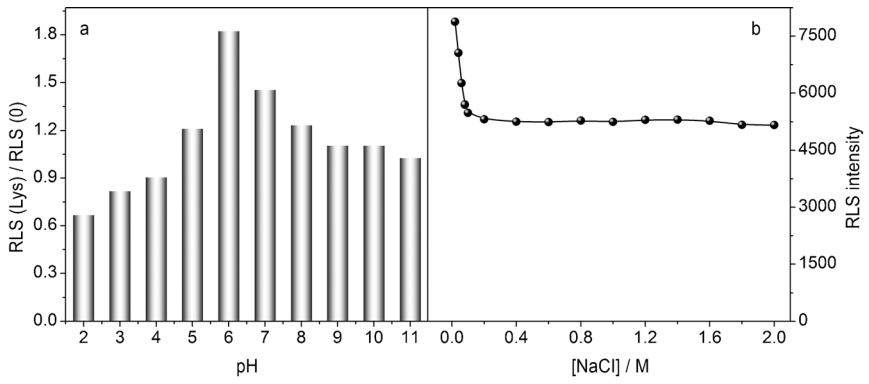

Figure 5. The influence of a) pH and b) ionic strength on the RLS assay for lysozyme (100 nM); pH 6 PBS buffer containing 0.2 M NaCl.

Application of RLS for study of BSA–lysozyme binding stoichiometry: In addition to biosensing of analytes, RLS has also been employed for studies of bimolecular interactions.[27] The protein–protein interaction is involved in many of the most important molecular processes in the cell, which is at the core of the entire interatomic system of any living cell. In this work, we found that the RLS assay was also potentially useful for studying the BSA–lysozyme

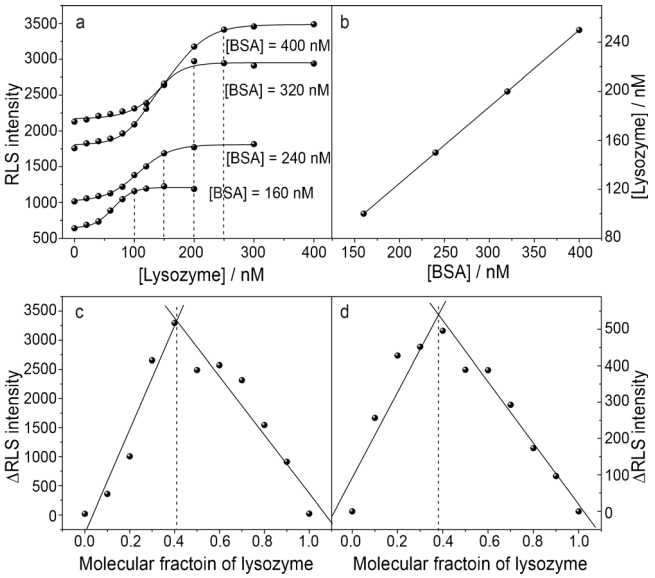

Figure 6. a) Saturation of the RLS intensity of dBSA-coated Mn-doped ZnS QDs when increasing the concentration of lysozyme. b) Correlation of the concentrations of BSA (as dBSA-coated Mn-doped ZnS QDs) and lysozyme; pH 6 PBS buffer containing 0.2 M NaCl. c) Job plot for the binding of lysozyme with BSA in the system involving QDs, and d) Job plot for the binding of lysozyme with BSA without QDs.

binding stoichiometry. As shown in Figure 6a, the RLS intensity of dBSA-coated Mn-doped ZnS QDs increased to a plateau when increasing the lysozyme concentrations, irrespective of the concentrations of QDs (here referred to as the concentration of BSA). However, the critical concentrations of lysozyme for these plateaus were proportional to the concentrations of QDs (Figure 6b). That is, when the concentrations of BSA were 160, 240, 320, and 400 nM, the critical concentrations of lysozyme were 100, 150, 200, and 250 nM, respectively. As a result, the binding stoichiometry for BSA and lysozyme was calculated to be 8:5 (Figure 6b), which corresponds to a lysozyme molar fraction of 0.38 in BSA–lysozyme complex. At a given concentration of QDs (which corresponds to a given concentration of BSA), the number of binding sites available for lysozyme is fixed. After saturation of the binding sites by lysozyme, no more aggregates of the QDs can be generated, thus leading to saturated RLS intensity.

To verify such stoichiometry obtained by the proposed method, Job plots were constructed by varying the concentration ratios of lysozyme to BSA (either as dBSA-coated Mn-doped ZnS QDs, or BSA alone) at a constant total molar concentration with RLS as readout (see the Supporting Information). Lysozyme molar fractions of 0.41 and 0.39 were obtained in the systems of QDs (Figure 6c) and BSA alone (Figure 6d), respectively. The binding stoichiometry of BSA and lysozyme calculated from the saturation point of the calibration curve by using dBSA-coated Mn-doped ZnS QDs as the RLS probe is thus in good agreement with that obtained from the Job plots.

For studying protein–protein interactions and binding stoichiometry, fluorescence correlation spectroscopy (FCS) is frequently used,[28] but expensive laser sources are required. Our research results provide an interesting yet simple and inexpensive alternative for studying protein–protein binding stoichiometry.

Conclusion

In summary, we have reported a protein-templated synthesis of Mn-doped ZnS QDs by employing BSA as the template. The protein-capped Mn-doped ZnS QDs could favor further biological applications such as biosensing and bioimaging, since they can be kept stable in up to 1 M NaCl media and provide multiple functional groups to further bioconjugation. The protein-assisted synthetic strategy also provides great potential for biosensor design, because the protein serves not only as the template for growth of Mn-doped ZnS QDs, but also as recognition sites for analytes. Through integration of the optical properties of Mn-doped ZnS QDs and recognition of analyte proteins by BSA, a dual-channel sensing system for proteins with dBSA-templated Mn-doped ZnS QDs was developed: phosphorescent quenching sensing of trypsin and RLS sensing of lysozyme. The proposed detection protocols provide high sensitivity and excellent selectivity. The developed synthesis protocol is expected to be extended to other functional proteins such as enzymes and antibodies/antigens to obtain novel bio/nanoconjugates for advanced bioapplications.

Experimental Section

Materials: All reagents used in this work were of at least analytical grade. BSA (Sigma–Aldrich); and MPA, $ZnAc_2{\cdot}7H_2O$, $MnAc_2{\cdot}4H_2O$, and $Na_2S{\cdot}9H_2O$ (Aladin, Shanghai, China) were used for preparation of Mn-doped ZnS QDs. Trypsin and glucose oxidase were purchased from Sigma–Aldrich. Lysozyme, papain, pepsin, HSA, ovalbumin, and transferrin were obtained from Newprobe Biotechnology Co., Beijing, China. Ultrapure water (18.2 $M\Omega\,cm^{-1}$) was obtained from a water purification system (ULUPURE, Chengdu, China).

Synthesis of Mn-doped ZnS QDs: Denatured BSA was prepared by chemically treating BSA with $NaBH_4$.[29] First, BSA (4.14 g) was dissolved in ultrapure water (60 mL), and additional $NaBH_4$ (0.4 g) was added as a reductant into the solution under stirring. The reaction proceeded at room temperature until no more gas was generated. Under these conditions, BSA was denatured, and most of its disulfide bonds were converted to sulfhydryl groups. The final concentration of dBSA aqueous solution was $1.0\times10^{-3}\,mol\,L^{-1}$. For preparation of Mn-doped ZnS QDs, dBSA (1 mL) and cation precursor ($Zn^{2+}+Mn^{2+}$; 0.25 mmol) were mixed; the final volume of the solution was 19 mL. Immediately after mixing dBSA with the cation precursor, a white precipitate formed. The pH of the mixed solution was adjusted to 9 (after disappearance of the precipitate) with NaOH (2 M). After bubbling with Ar for 20 min, Na_2S solution (1 mL, 0.25 M) was added. Then, the reaction solution was aged at 70 °C for 3 h to obtain dBSA-coated Mn-doped ZnS QDs. For purification of the QDs for characterization, they were subjected to acetone precipitation and centrifuged, then vacuum dried.

Characterization: Fluorescence, phosphorescence, phosphorescence lifetime, and RLS measurements were performed using an F-7000 spectro-

fluorometer (Hitachi, Japan) equipped with a plotter unit and a quartz cell (1 cm × 1 cm). For RLS measurements, the voltage of the photomultiplier tube (PMT) was set at 400 V, whereas for the rest of the measurements it was 700 V. Absorption spectra were recorded using a UV-1700 UV/Vis spectrophotometer (Shimadzu, Japan). The excitation wavelength for fluorescence, phosphorescence, and phosphorescence lifetime measurements was set at 280 nm. The RLS spectra were recorded by scanning the excitation and emission monochromators simultaneously ($\Delta\lambda = 0$) from 200 to 500 nm. HRTEM images of QDs were obtained using a Tecnai G2 F20 S-TWIN transmission electron microscope at an accelerating voltage of 200 kV (FEI Co., USA). X-ray diffraction (XRD) spectra were collected using an X'Pert Pro MPD X-ray diffractometer (Philips, Netherlands) with $Cu_{K\alpha}$ radiation. FTIR and FT-Raman spectra were collected using a Nicolet IS10 FTIR spectrometer (Thermo Inc., America) and an HR800 FT-Raman spectrometer (Horiba JY, Japan). The elemental concentration was measured with an inductively coupled plasma atomic emission spectrometer (SPECTRO ARCOS, Germany).

Acknowledgements

This work was supported by the National Natural Science Foundation of China (nos. 20835003 and 21145002) and startup funding from Sichuan University for P.W. (YJ 2011-015). The kind assistance of HRTEM measurements by Dr. Shanlin Wang of the Analytical & Testing Center, Sichuan University was greatly appreciated.

[1] a) E. Katz, I. Willner, *Angew. Chem.* **2004**, *116*, 6166–6235; *Angew. Chem. Int. Ed.* **2004**, *43*, 6042–6108; b) N. L. Rosi, C. A. Mirkin, *Chem. Rev.* **2005**, *105*, 1547–1562.

[2] a) J. Kalia, R. T. Raines, *Curr. Org. Chem.* **2010**, *14*, 138–147; b) R. A. Sperling, W. J. Parak, *Philos. Trans. R. Soc. London Ser. A* **2010**, *368*, 1333–1383.

[3] a) M. B. Dickerson, K. H. Sandhage, R. R. Naik, *Chem. Rev.* **2008**, *108*, 4935–4978; b) S. S. Behrens, *J. Mater. Chem.* **2008**, *18*, 3788–3798; c) W. J. Crookes-Goodson, J. M. Slocik, R. R. Naik, *Chem. Soc. Rev.* **2008**, *37*, 2403–2412.

[4] a) L. Saa, A. Virel, J. Sanchez-Lopez, V. Pavlov, *Chem. Eur. J.* **2010**, *16*, 6187–6192; b) J. P. Xie, Y. G. Zheng, J. Y. Ying, *J. Am. Chem. Soc.* **2009**, *131*, 888–889; c) J. Ge, J. Lei, R. N. Zare, *Nat. Nanotechnol.* **2012**, *7*, 428–432.

[5] a) B. Adhikari, A. Banerjee, *Chem. Eur. J.* **2010**, *16*, 13698–13705; b) Y. N. Tan, J. Y. Lee, D. I. C. Wang, *J. Am. Chem. Soc.* **2010**, *132*, 5677–5686; c) K. A. Gattás-Asfura, R. M. Leblanc, *Chem. Commun.* **2003**, 2684–2685; d) J. M. Slocik, J. S. Zabinski, D. M. Phillips, R. R. Naik, *Small* **2008**, *4*, 548–551.

[6] a) G. Tikhomirov, S. Hoogland, P. E. Lee, A. Fischer, E. H. Sargent, S. O. Kelley, *Nat. Nanotechnol.* **2011**, *6*, 485–490; b) N. Ma, E. H. Sargent, S. O. Kelley, *Nat. Nanotechnol.* **2009**, *4*, 121–125; c) L. Berti, G. A. Burley, *Nat. Nanotechnol.* **2008**, *3*, 81–87.

[7] a) N. Ma, C. J. Dooley, S. O. Kelley, *J. Am. Chem. Soc.* **2006**, *128*, 12598–12599; b) L. A. Gugliotti, D. L. Feldheim, B. E. Eaton, *J. Am. Chem. Soc.* **2005**, *127*, 17814–17818.

[8] Y. C. Wang, Y. Wang, F. B. Zhou, P. Kim, Y. N. Xia, *Small* **2012**, *8*, 3769–3773.

[9] a) D. Liu, M. Y. Liu, G. H. Liu, S. C. Zhang, Y. Y. Wu, X. R. Zhang, *Anal. Chem.* **2010**, *82*, 66–68; b) J. Hu, X. M. Jiang, L. Wu, K. L. Xu, X. D. Hou, Y. Lv, *Anal. Chem.* **2011**, *83*, 6552–6558.

[10] a) R. Thakar, Y. C. Chen, P. T. Snee, *Nano Lett.* **2007**, *7*, 3429–3432; b) Y. He, H.-F. Wang, X.-P. Yan, *Anal. Chem.* **2008**, *80*, 3832–3837; c) R. Y. Tu, B. H. Liu, Z. Y. Wang, D. M. Gao, F. Wang, Q. L. Fang, Z. P. Zhang, *Anal. Chem.* **2008**, *80*, 3458–3465; d) P. Wu, Y. He, H.-F. Wang, X.-P. Yan, *Anal. Chem.* **2010**, *82*, 1427–1433; e) D. Zhu, Y. Chen, L.-p. Jiang, J. Geng, J.-R. Zhang, J.-J. Zhu, *Anal. Chem.* **2011**, *83*, 9076–9081; f) W.-S. Zou, D. Sheng, X. Ge, J.-Q. Qiao, H.-Z. Lian, *Anal. Chem.* **2011**, *83*, 30–37.

[11] a) P. Wu, L.-N. Miao, H.-F. Wang, X.-G. Shao, X.-P. Yan, *Angew. Chem.* **2011**, *123*, 8268–8271; *Angew. Chem. Int. Ed.* **2011**, *50*, 8118–8121; b) H. Yan, H.-F. Wang, *Anal. Chem.* **2011**, *83*, 8589–8595.

[12] W. B. Zhou, F. Baneyx, *ACS Nano* **2011**, *5*, 8013–8018.

[13] a) M. S. Bakshi, P. Thakur, G. Kaur, H. Kaur, T. S. Banipal, F. Possmayer, N. O. Petersen, *Adv. Funct. Mater.* **2009**, *19*, 1451–1458; b) L. Au, B. Lim, P. Colletti, Y. S. Jun, Y. N. Xia, *Chem. Asian J.* **2010**, *5*, 123–129; c) D. Ghosh, S. Mondal, S. Ghosh, A. Saha, *J. Mater. Chem.* **2012**, *22*, 699–706.

[14] C. B. Murray, C. R. Kagan, M. G. Bawendi, *Annu. Rev. Mater. Sci.* **2000**, *30*, 545–610.

[15] a) Y. M. Chen, C. J. Yu, T. L. Cheng, W. L. Tseng, *Langmuir* **2008**, *24*, 3654–3660; b) Y. U. Moon, R. A. Curtis, C. O. Anderson, H. W. Blanch, J. M. Prausnitz, *J. Solution Chem.* **2000**, *29*, 699–717.

[16] a) G. M. Dalpian, J. R. Chelikowsky, *Phys. Rev. Lett.* **2006**, *96*, 226802; b) D. J. Norris, A. L. Efros, S. C. Erwin, *Science* **2008**, *319*, 1776–1779.

[17] J. F. Suyver, S. F. Wuister, J. J. Kelly, A. Meijerink, *Nano Lett.* **2001**, *1*, 429–433.

[18] H. S. M. H. S. Mansur, J. C. González, A. A. P. Mansur, *Colloids Surf. B* **2011**, *84*, 360–368.

[19] M. S. Wolfe, *Chem. Rev.* **2009**, *109*, 1599–1612.

[20] a) M. F. Byrne, R. M. Mitchell, H. Stiffler, P. S. Jowell, M. S. Branch, T. N. Pappas, D. Tyler, J. Baillie, *Can. J. Gastroenterol.* **2002**, *16*, 849–854; b) P. G. Lankisch, S. Burchard-Reckert, D. Lehnick, *Gut* **1999**, *44*, 542–544.

[21] a) I. L. Medintz, A. R. Clapp, F. M. Brunel, T. Tiefenbrunn, H. T. Uyeda, E. L. Chang, J. R. Deschamps, P. E. Dawson, H. Mattoussi, *Nat. Mater.* **2006**, *5*, 581–589; b) L. F. Shi, V. De Paoli, N. Rosenzweig, Z. Rosenzweig, *J. Am. Chem. Soc.* **2006**, *128*, 10378–10379; c) C.-W. Liu, H.-T. Chang, *Open Anal. Chem. J.* **2007**, *1*, 1–6.

[22] W. A. See, J. L. Smith, *Transplantation* **1991**, *52*, 630–633.

[23] J. Ling, C. Z. Huang, Y. F. Li, L. Zhang, L. Q. Chen, S. J. Zhen, *TrAC Trends Anal. Chem.* **2009**, *28*, 447–453.

[24] S. Perera, M. Uddin, J. A. Hayes, *Int. J. Reliab. Qual. Saf. Eng. Int. J. Behav. Med.* **1997**, *4*, 170–178.

[25] a) T. Li, L. B. Zhang, J. Ai, S. J. Dong, E. K. Wang, *ACS Nano* **2011**, *5*, 6334–6338; b) S. Bamrungsap, M. I. Shukoor, T. Chen, K. Sefah, W. H. Tan, *Anal. Chem.* **2011**, *83*, 7795–7799; c) X. Q. Qian, Y. Xiang, H. X. Zhang, Y. Chen, Y. Q. Chai, R. Yuan, *Chem. Eur. J.* **2010**, *16*, 14261–14265.

[26] N. K. Howell, N. A. Yeboah, D. F. V. Lewis, *Int. J. Food Sci. Technol.* **2007**, *30*, 813–824.

[27] a) M. H. Xiang, X. Xu, F. Liu, N. Li, K. A. Li, *J. Phys. Chem. B* **2009**, *113*, 2734–2738; b) R. F. Pasternack, C. Bustamante, P. J. Collings, A. Giannetto, E. J. Gibbs, *J. Am. Chem. Soc.* **1993**, *115*, 5393–5399; c) S. C. M. Gandini, V. E. Yushmanov, I. E. Borissevitch, M. Tabak, *Langmuir* **1999**, *15*, 6233–6243; d) R. F. Pasternack, E. J. Gibbs, D. Bruzewicz, D. Stewart, K. S. Engstrom, *J. Am. Chem. Soc.* **2002**, *124*, 3533–3539.

[28] a) B. Wu, Y. Chen, J. D. Muller, *Proc. Natl. Acad. Sci. USA* **2010**, *107*, 4117–4122; b) Y. Chen, J. D. Muller, *Proc. Natl. Acad. Sci. USA* **2007**, *104*, 3147–3152.

[29] Q. Wang, Y. C. Kuo, Y. W. Wang, G. Shin, C. Ruengruglikit, Q. R. Huang, *J. Phys. Chem. B* **2006**, *110*, 16860–16866.

Received: November 11, 2012
Published online: ■■ ■■, 0000

Quantum Dots

*P. Wu, T. Zhao, Y. F. Tian, L. Wu, X. D. Hou** ..... ■■■■–■■■■

Protein-Directed Synthesis of Mn-Doped ZnS Quantum Dots: A Dual-Channel Biosensor for Two Proteins

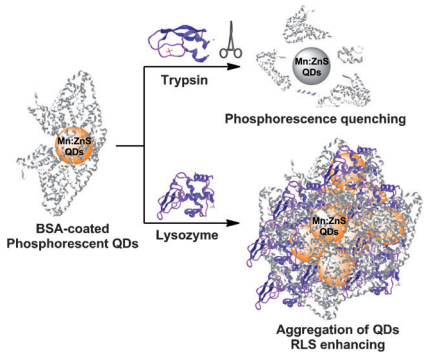

2 proteins, 1 sensor: Protein-directed synthesis of phosphorescent Mn-doped ZnS quantum dots (QDs) is reported. By exploring the phosphorescence and resonance light scattering (RLS) of the QDs, and the specific protein–protein interactions with bovine serum albumin (BSA) as the substrate, a dual-channel sensor was developed that employs only one type of QDs for the detection of two different proteins (see figure).